Energy Conversion and Management 270 (2022) 116248

Contents lists available at ScienceDirect

Energy Conversion and Management

journal homepage: www.elsevier.com/locate/enconman

Carbon-negative hydrogen from biomass using gas switching integrated gasification: Techno-economic assessment

Antonia Helf [a], Schalk Cloete [b], Florian Keller [a], Jan Hendrik Cloete [b], Abdelghafour Zaabout [b,*]

[a] TU Bergakademie Freiberg, Institute of Energy Process Engineering and Chemical Engineering, Germany
[b] Process Technology Department, SINTEF Industry, Norway

ARTICLE INFO

Keywords:
Hydrogen
Biomass
CO_2 capture
Gasification
Negative emissions
Chemical looping

ABSTRACT

Ambitious decarbonization pathways to limit the global temperature rise to well below 2 °C will require large-scale CO_2 removal from the atmosphere. One promising avenue for achieving this goal is hydrogen production from biomass with CO_2 capture. The present study investigates the techno-economic prospects of a novel biomass-to-hydrogen process configuration based on the gas switching integrated gasification (GSIG) concept. GSIG applies the gas switching combustion principle to indirectly combust off-gas fuel from the pressure swing adsorption unit in tubular reactors integrated into the gasifier to improve efficiency and CO_2 capture. In this study, these efficiency gains facilitated a 5% reduction in the levelized cost of hydrogen (LCOH) relative to conventional O_2-blown fluidized bed gasification with pre-combustion CO_2 capture, even though the larger and more complex gasifier cancelled out the capital cost savings from avoiding the air separation and CO_2 capture units. The economic assessment also demonstrated that advanced gas treatment using a tar cracker instead of a direct water wash can further reduce the LCOH by 12% and that the CO_2 prices in excess of 100 €/ton, consistent with ambitious decarbonization pathways, will make this negative-emission technology economically highly attractive. Based on these results, further research into the GSIG concept to facilitate more efficient utilization of limited biomass resources can be recommended.

1. Introduction

According to the recent Sixth Assessment Report from the IPPC [1], it is now unequivocal that human activity has led to global warming, which is already affecting weather and climate extremes around the planet. Following the Paris Agreement in 2015 to limit global warming to well below 2 °C, there has been increasing international action to reduce anthropogenic greenhouse gas emissions to limit the future impacts of climate change. An increasing number of countries are committing to net-zero emissions by 2050 or shortly after, driving tangible decarbonization efforts around the world.

While there are many roads to decarbonization, hydrogen is expected to be part of the solution as an important carbon-free energy carrier in sectors such as industry and transport [2]. The latest Energy Technology Perspectives report from the IEA [3] estimates the production of hydrogen to increase from 75 Mt/year in 2019 to 520 Mt/year in 2070. However, at present hydrogen is almost exclusively produced from fossil fuels with large CO_2 emissions. Therefore, such widespread use of hydrogen would require the rapid deployment of low-carbon hydrogen technologies, including hydrogen from fossil fuels with carbon capture and storage [4], from water electrolysis [5] using renewable and nuclear electricity, or from natural gas pyrolysis [6].

While these low-carbon hydrogen technologies will play an important role in the energy transition, there is an increasing consensus that negative emission technologies (NETs) will also be required to compensate for hard-to-abate CO_2 emissions and for an eventual overshoot of the remaining carbon budget set for meeting global warming targets [7,8]. Direct air capture (DAC) and storage of CO_2 is an option [9], but the low concentration of CO_2 in the atmosphere makes it energy- and capital-intensive. An alternative approach is bioenergy with carbon capture and storage (BECCS) [10]. Producing hydrogen as a carbon-free fuel from biomass is especially promising as a negative emission pathway, since it has the potential to sequester the maximum amount of carbon from a given amount of biomass. However, there are limits to the amount of biomass that can be produced sustainably [11] and irresponsible deployment of BECCS could even have a negative effect on planetary boundaries other than climate change [12]. It therefore becomes increasingly important to develop highly efficient technologies to maximise both the energy produced and the CO_2 captured from this

* Corresponding author at: Flow Technology Group, SINTEF Industry, S.P. Andersens vei 15 B, 7031 Trondheim, Norway.
E-mail address: abdelghafour.zaabout@sintef.no (A. Zaabout).

https://doi.org/10.1016/j.enconman.2022.116248
Received 12 June 2022; Received in revised form 13 September 2022; Accepted 14 September 2022
Available online 22 September 2022

List of Acronyms

ACF	Annualized cash flow
AGR	Acid gas removal
ASU	Air separation unit
BEC	Bare erected cost
BECCS	Bioenergy with CO_2 capture and storage
DAC	Direct air capture
EPC	Engineering, procurement, and construction
ETS	EU Emissions Trading System
GSC	Gas switching combustion
GSIG	Gas switching integrated gasification
GSR	Gas switching reforming
HEX	Heat exchanger
HTW	High temperature Winkler
IEA	International Energy Agency
IPCC	Intergovernmental Panel on Climate Change
LCOH	Levelized cost of hydrogen
LHV	Lower heating value
Mt	Megaton
NET	Negative emission technology
NPV	Net present value
OC	Owner's cost
PC	Project contingency
PSA	Pressure swing adsorption
SEA	Standardized economic assessment
S/B	Steam/biomass (by mass)
TOC	Total overnight cost

limited resource.

Biomass can be converted to hydrogen through thermochemical, biological, and electrochemical processes, with thermal gasification being the preferred option for large-scale processes and high hydrogen yields [13]. High-grade heat is required to drive the endothermic gasification reactions, and the process can be classified as direct or indirect gasification based on how this heat is provided. In direct gasification, air or oxygen is directly added to the gasifier to combust a portion of the biomass, producing the required heat. However, combustion with air dilutes to syngas with nitrogen, increasing the cost of hydrogen separation and CO_2 capture. Combustion with oxygen, on the other hand, adds significant cost due to required air separation unit (ASU). Consequently, indirect gasification [14] becomes an attractive alternative for hydrogen production with CO_2 capture. One option is to utilize a dual circulating fluidized bed reactor, where the char is combusted with air and the heat is transferred to the gasifier by circulating an inert powder [15]. However, scale up of such a circulating fluidized bed concept will be challenging at high pressure operating conditions, required for efficient hydrogen production with CO_2 capture [16] and the combustion of char with air produces a CO_2 stream diluted with nitrogen, raising CO_2 capture costs. An alternative is to separately combust a portion of the fuel and transfer the heat to the gasifier by means of heat exchanger tubes [17]. However, this process is hampered by the low heat transfer coefficients of the flue gases, requiring other measures to reduce the need for large heat transfer areas which adds to the gasifier cost [18].

Thermochemical hydrogen production processes such as gasification typically involve a pressure swing adsorption (PSA) unit for hydrogen separation from the shifted syngas [19]. In such processes, efficient utilization of the low-grade PSA off-gas fuel is of importance to achieve a high overall process efficiency. Although this fuel can be combusted to raise steam for a relatively low efficiency Rankine cycle [20], a far more efficient solution is to combust the PSA off-gas fuel to provide the heat for the endothermic gasification process [21], mimicking the typical arrangement in steam methane reforming (SMR) hydrogen plants. However, carrying out gasification with pressurized solid fuel feeding and ash removal in a large number of tubes within a furnace (as in SMR) is unlikely to be technically feasible.

Another challenge is to economically capture CO_2, either via pre-combustion capture before the PSA or oxyfuel or post-combustion capture afterwards. Chemical looping technologies [22] have consequently attracted large research interest due to their potential to minimize the energy penalty of CO_2 capture by means of inherent CO_2 separation. This is achieved by alternating an oxygen carrier material between oxidation and reduction steps, preventing mixing of nitrogen from air and CO_2-containing flue gas. Numerous processes have been proposed to integrate chemical looping with biomass gasification [23], relying on the oxygen carrier to transport the heat generated during oxidation to the gasifier. However, these processes face challenges related to oxygen carrier deactivation during direct contact with biomass, reduced CO_2 capture efficiencies due to transport of unconverted char to the air reactor along with the circulating oxygen carrier, as well as scale–up of the processes relying on circulating fluidized bed reactors under pressurized conditions [24].

Gas switching technology has been proposed as a promising alternative for application of the chemical looping principle in pressurized applications [25]. Here, the oxygen carrier is maintained in a single bubbling fluidized bed reactor, only alternating the gas feed to switch between the oxidation and reduction steps. This approach eliminates the challenge of achieving reliable solids circulation under pressurized conditions, and it has been experimentally demonstrated under pressurized conditions [26,27] in a concept called gas switching combustion (GSC). Several studies have investigated the integration of GSC technology in low-carbon solid fuel power plants for large efficiency gains relative to conventional benchmarks [28–30], with techno-economic assessments showing CO_2 avoidance costs as low as 22 €/ton [31] with further benefits available from flexible electricity and hydrogen production [32] for balancing variable renewables. Alternatively, it has been shown experimentally that gas switching technology can be employed for efficient low-carbon hydrogen production from methane via gas switch reforming (GSR) by using the heat from the combustion steps in the endothermic reforming step [33]. Techno-economic assessments have shown that GSR can achieve similarly low CO_2 avoidance costs (15 $/ton) for low-carbon hydrogen production [34] and that flexible power and hydrogen production also presents an attractive possibility in this application [35,36].

Considering the above status of chemical looping technologies and biomass gasification to produce hydrogen with carbon capture, the present paper presents a novel technology, the gas switching integrated gasifier (GSIG), for efficient conversion of biomass to hydrogen with high CO_2 capture rates to deliver large negative emissions. Using the GSC principle, the aim of GSIG is to efficiently integrate the PSA off-gas to provide the heat for gasification, while achieving inherent CO_2 separation and high heat transfer coefficients. Simultaneously, GSIG avoids the challenges associated with pressurized solids circulation and direct mixing of the oxygen carrier with the biomass. In the following, the GSIG concept is first described in detail, for the first time showing how GSC can be integrated in an indirect biomass gasification process. Subsequently, it is techno-economically benchmarked against a conventional process for biomass-to-hydrogen with CO_2 capture to evaluate the potential of the innovative GSIG concept.

2. The gas switching integrated gasifier

Fig. 1 illustrates the principle of the GSIG concept. Essentially, it is a bubbling fluidized bed gasifier designed as a shell-and-tube heat exchanger where the gasification happens on the shell side and heating

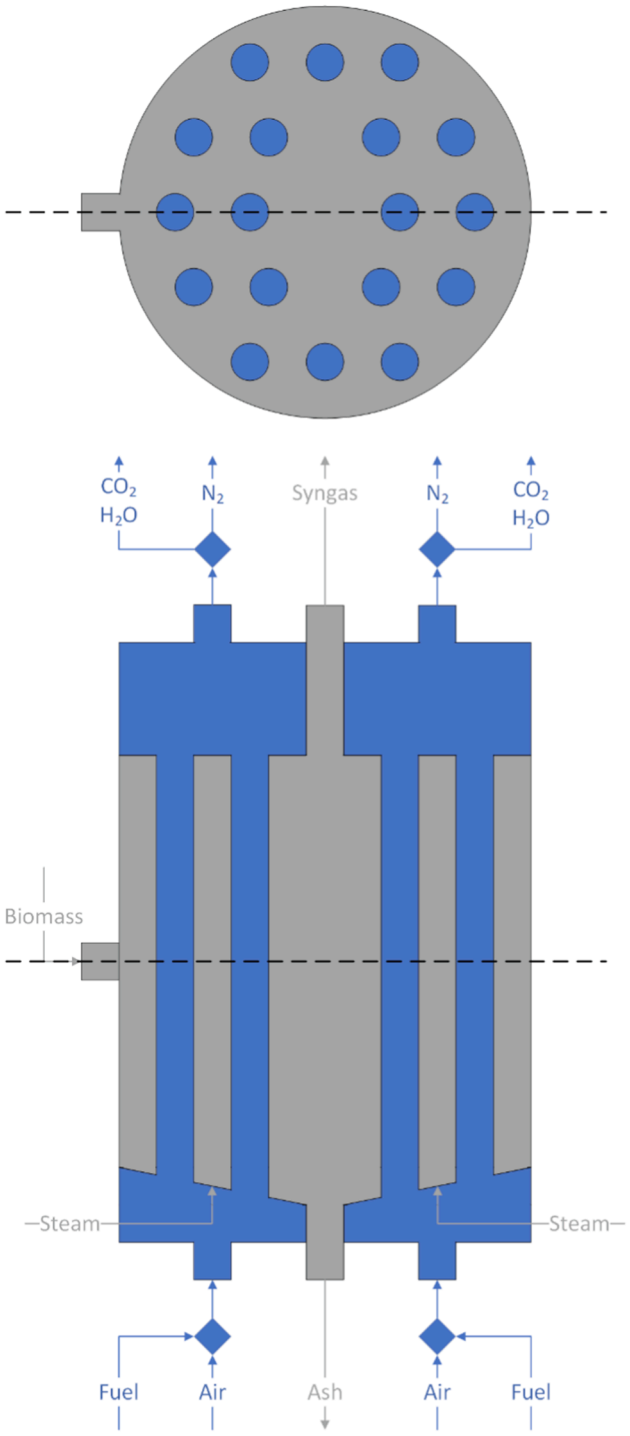

Fig. 1. Simple illustration of the GSIG concept from a top and front view. The grey parts represent the gasifier and the blue parts the GSC reactors.

is supplied within the tubes operated as GSC reactors. The GSC reactor tubes, which facilitate combustion of the PSA off-gas fuel without mixing of CO_2 and N_2, are joined together via chambers at the top and the bottom. The bottom chamber ensures that gas can be supplied to multiple tubes via a single sparger and inlet control valve. Similarly, the top chamber joins together several tubes to a single outlet and control valve and also serves as an expanding freeboard to avoid oxygen carrier elutriation. As shown in Fig. 1, the top and bottom chambers are split into several sections, each connecting multiple GSC tubes, so that these dynamically operated units can approximate steady operation, i.e., fuel can be fed to one section and air to another at any given moment in the dynamic operating cycle.

Although the GSC concept is proven in a single reactor, the ability to equally fluidize multiple tubes connected by a chamber at the bottom and the top remains to be demonstrated. However, if the tubes are wide enough, the natural tendency for the static pressure to equilibrate should make it impossible for gas to short-circuit through one tube while the others are blocked with stagnant solids. The tube diameter of 30 cm that emerged in the techno-economic assessment in this study should be wide enough to ensure that the plug-like fluidization behaviour required for short-circuiting is not possible.

Another potential challenge is related to fouling of the tube surfaces, causing reductions in the heat transfer rate. In this respect, the constant abrasion caused by the fluidized particles should have a self-cleaning effect, avoiding this problem. It might be necessary to have a hard fluidized medium (like silica sand) in the gasifier chamber to ensure that the outside of the tubes stay clean.

Furthermore, the dynamic nature of the GSC operation can cause significant transient temperature fluctuations in the heating tubes. However, if an oxygen carrier material with exothermic reduction reactions (e.g., Cu-based or Mn-based) is used, heat will be released both during reduction and oxidation, minimizing temperature variations across the cycle. Furthermore, the reactor will be operated so that there are always some tubes in oxidation and others in reduction. Hence, if the oxidation temperature is slightly above average and the reduction temperature slightly below, the average heat transfer rate from the GSC tubes to the gasifier will not be significantly affected.

The potential for leakage of air from the tubes into the gasification chamber presents another risk. Here, the fact that the gasifier and GSC tubes will be operated at the same pressure will help to minimize the likelihood of such leaks occurring. Furthermore, the likelihood of a large leak that poses an explosion risk would be very low with a negligible pressure difference between the gasifier and the GSC tubes.

3. Methodology

3.1. Process modelling

The process and the GSIG reactor are modelled using Aspen Plus, employing the Peng-Robinson equation of state with Boston-Mathias modifications, to efficiently integrate the solid biomass into the model. This is achieved in the commonly applied way of using a "RYield" conversion block to decompose the biomass, a so-called "non-conventional component", with known heating value and elemental analysis (see Table 1 for data) into pure elemental components according to the mass distribution. The heat that this conversion requires is taken from the following gasification reactor. This allows Aspen Plus to calculate enthalpies, equilibriums and reactions based on these pure components. The biomass is transported into the pressurized reactor by a lock hopper system that uses CO_2 as a pressurizing agent. Some of this CO_2 is lost to the environment with each loading, some enters the reactor alongside the biomass and some can be recycled (see Table 2 for distribution).

Throughout the whole modelling process, heat integration plays a major part as it is necessary to raise a sufficient amount of process steam

Table 1
Elemental analysis of the biomass (beech wood) selected for this study.

Element	wt.-% (dry)
C	49.95
O	43.56
H	6.11
N	0.22
S	0.15

Table 2
Parameter for modelling.

Parameter	Unit	Value
Biomass input	kg/s	15
Input temperature for water and biomass	°C	15
Process pressure (pressure of gasifier)	bar	25
Temperature approach in gas–gas HEX [16]	°C	20
Temperature approach in liquid–gas and condensation HEX [16]	°C	10
Pressure loss in heat exchangers for gases [16]	%	2
Pressure loss in heat exchangers for liquids [16]	bar	0.4
Pressure loss in PSA [16]	%	1
Pressure loss in gasifier	bar	0.5
Steam pressure levels HP/IP/LP	bar	110/25/0.15
Steam temperature HP/IP	°C	550/225
Cooling water temperature difference/pressure [16]	°C/bar	12/2.92
Pump efficiencies water/CO_2 [16]	%	70/75
Turbine efficiencies steam HP/IP/LP [16]	%	94/92/88
Turbine efficiencies N_2 [16]	%	92.5
Compressor efficiencies air/other gases [16]	%	92.5/80
CO_2 flow for lock hoppers [37]	kg/s	2.25
Distribution of CO_2 to reactor/recycled/lost [37]	%	0.3/0.6/0.1
Power demand of ASU [38]	kWh/t_{O2}	354
ASU O_2 purity [38]	%	98
Power demand of Rectisol [38]	kWh/kg_{CO2}	0.044
Heat demand of Rectisol [38]	kWh/kg_{CO2}	0.058
CO_2 in Rectisol outlet gas	mol%	0.7
Ratio of quench water to dry gas	–	4
Ratio of pressure wash water to dry gas	–	8
CO_2 output pressure [16]	bar	115
H_2 output pressure	bar	60

and also use excess heat as efficiently as possible. This is achieved by adding a steam turbine cycle. All steam that is generated by cooling product gas streams and is raised at a pressure well above the process pressure. A high-, intermediate- and low-pressure turbine are added to generate power. The process steam is extracted before the intermediate-pressure turbine. Low-grade heat that cannot be used within the process is rejected to cooling water. Parameters and efficiencies for turbines, pumps and other equipment are summarized in Table 2.

3.1.1. High temperature Winkler reference plant (HTW)

As a suitable reference for the plants designed around the GSIG concept, the standard HTW biomass gasification process shown in Fig. 2 is modelled. Biomass, O_2 from an ASU, and steam are sent to the gasifier modelled as a Gibbs free energy minimization reactor, operating at 850 °C and 25 bar. A fraction of 2% of carbon in the feed is assumed to be inert. The electricity consumption of the ASU is taken from literature (Table 2) as this unit is not incorporated explicitly in the process model, with the O_2 flowrate adjusted to achieve the targeted gasifier temperature.

Tar formation is not modelled directly, but syngas treatment steps are included to account for the effect of tar handling on the process. In this basic gas treatment configuration, the syngas emerging from the gasifier is quenched and then scrubbed with pressurized water to wash out any solid particles and other undesired components such as tars. This substantial process simplification downgrades a large amount of high-grade heat from the gasifier, which lowers process efficiency, although the extra steam introduced into the syngas stream promotes the subsequent water–gas shift (WGS) reaction.

After the scrubbing, the gas is cooled and sent to a two-step WGS (equilibrium reactor units) to transform most of the steam and CO present to hydrogen and CO_2. While sulfur-tolerant catalysts are readily available for the high temperature reactor, such catalysts have only become available more recently for the low temperature reactor and may require relatively large reactor volumes. The process layout in Fig. 2 assumes that modern WGS catalysts make low-temperature shift of a sulfur-containing syngas feasible from a technical and economic standpoint.

This 2-step WGS is followed by a Rectisol unit to separate H_2S and CO_2 from the shifted syngas. Thus, this is a pre-combustion capture of CO_2 that can only capture CO_2 that is produced in the gasification and shift reactions. The Rectisol process is modelled as a simple separator that extracts H_2S to a content of less than 1 ppm in the clean gas and CO_2 to about 0.7 mol-% in the clean gas. The energy demand for this process unit is estimated from literature values (Table 2) and the CO_2 captured in the Rectisol unit is compressed using a 3-stage CO_2 compression train. The Rectisol unit is then followed by the PSA, which is modelled as a simple separator with an off-gas pressure-dependent hydrogen recovery rate based on Nazir, Cloete [16], resulting in H_2 recoveries around 87% in the present study. The PSA produces a stream of pure hydrogen that is compressed to 60 bar for export. Additionally, a PSA off-gas is produced near atmospheric pressure, consisting of all other components.

The combustion of the PSA off-gas is modelled as another Gibbs reactor, with the heat used for steam generation. A significant amount of CO_2 is vented in the flue gas from the combustor, mainly originating from CH_4 generated in the gasifier. The S/B ratio is an influential optimization variable in the reference plant with a higher S/B ratio increasing H_2 production (due to less methane formation and more WGS) at the expense of higher electricity consumption (due to higher O_2 demand from the ASU and less PSA off gas for power production). In this case, an S/B ratio of 0.5 was found to result in a suitable balance in this trade-off.

3.1.2. GSIG with basic gas treatment (GSIG-B)

For a direct assessment of the effect of the GSIG concept, the simplified gas treatment in the reference plant is adapted to a GSIG plant illustrated in Fig. 3. The same biomass input is used, but steam is now the only gasification agent with heat supplied from GSC tubes instead of direct biomass combustion using O_2. The only difference from the HTW gas treatment described in the previous section is that only H_2S is removed after the quench and WGS reactors using a Selexol instead of a Rectisol process. CO_2 can be retained in the stream because it is inherently separated in the GSC tubes integrated into the gasifier.

The PSA off-gas (stream G10) is then recompressed and combusted with compressed air in another Gibbs reactor representing the GSC reactor tubes. This step is modelled to be stoichiometric and isothermal in order to represent the heat transfer from the GSC to the gasification. The reactor is set to a certain temperature (100 °C in the base case) above the gasification temperature (800 °C) to allow a significant driving force for heat flow from the GSC tubes to the gasifier. The resulting heat duty of the GSC reactor therefore represents the heat supply to the gasifier. The gasifier itself is modelled as a Gibbs reactor in the same way as in the reference plant.

Heat supply and demand in the GSIG unit are matched by changing the S/B ratio, which affects both the gasifier heat demand (more steam requires more heat to reach reactor temperatures and drives more endothermic reactions) and the GSC heat supply (more steam reduces methane in the syngas, lowering the amount of PSA off-gas fuel available for combustion in the GSC tubes). Thus, the S/B ratio cannot be freely varied as in the reference plant.

To simulate the behavior of the GSC tubes, the product gas from the combustion is separated into a nitrogen-rich oxidation stage gas (stream A05) and the reduction stage gas consisting mainly of CO_2 and steam (stream G12). However, the imperfect CO_2 capture in GSC due to the undesired mixing that takes place when switching between the two reactor steps is taken into account by mixing 3% of each stream into the other, based on earlier work [30].

The nitrogen-rich stream is expanded in a turbine and excess heat after the expansion is used in the heat integration. Similarly, all heat left in the reduction stage gas stream is integrated into the heat exchanger network. The stream is cooled to ambient temperatures for drying and

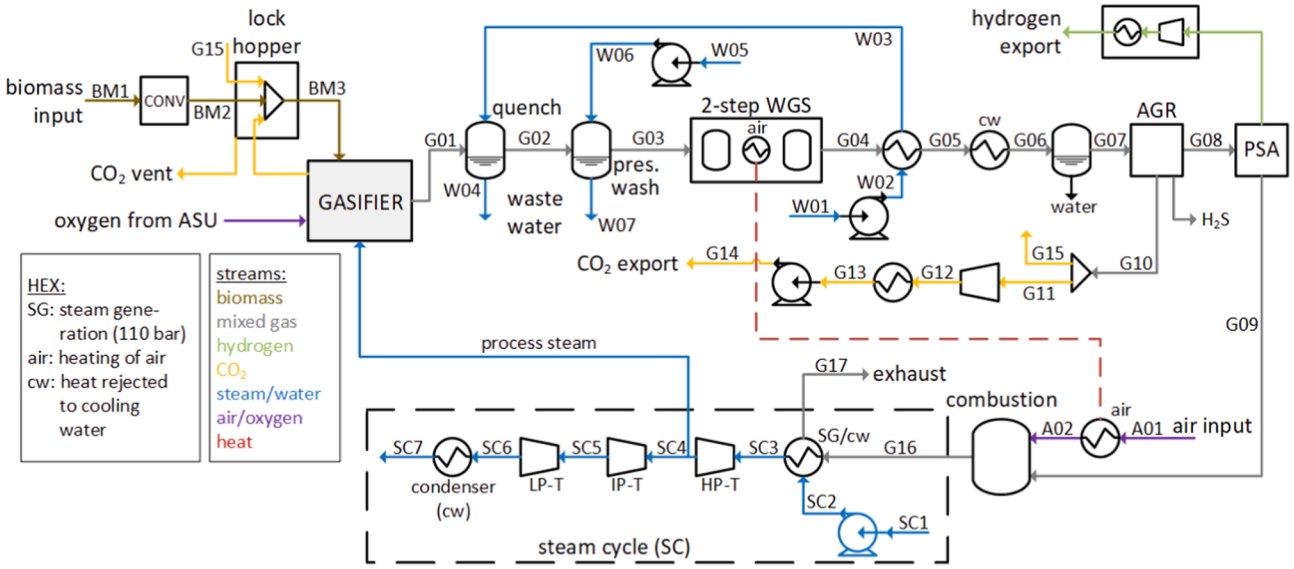

Fig. 2. Flow diagram of the reference HTW process.

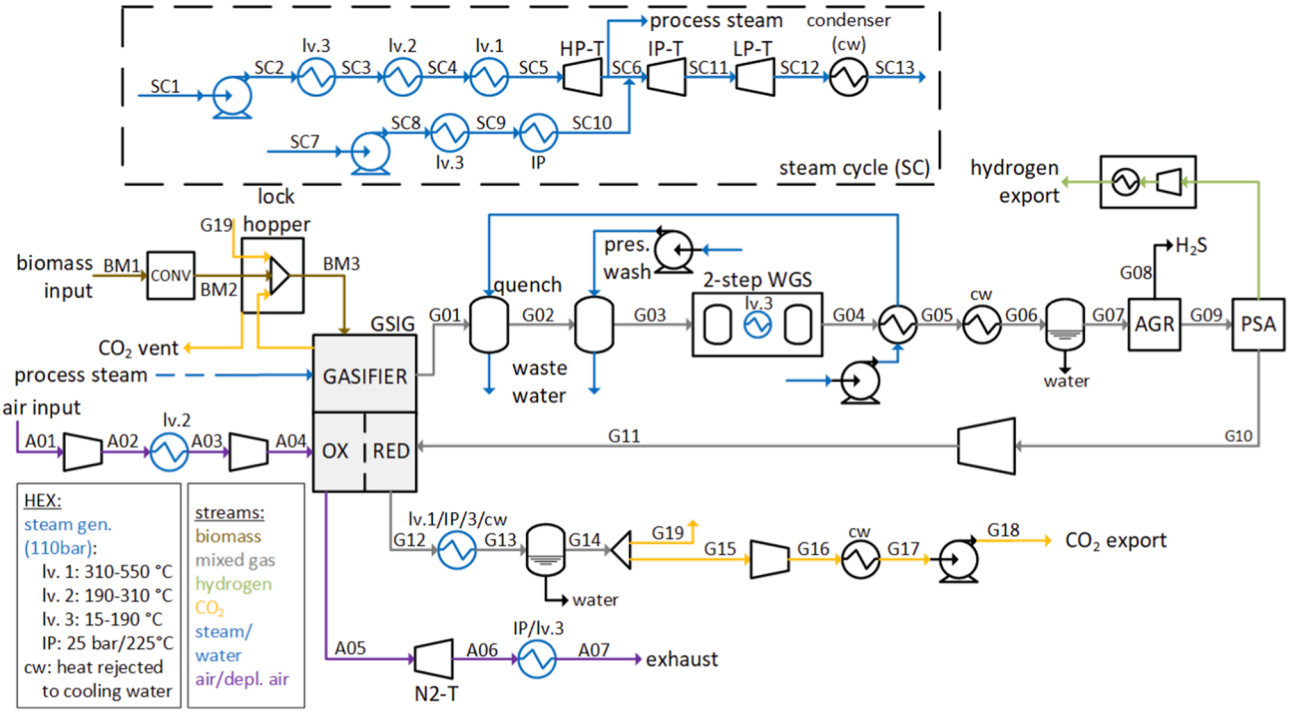

Fig. 3. Flow diagram of the GCIG process with basic gas treatment.

compressed to supercritical pressure before being pumped to the export pressure of 115 bar. A small fraction of the CO_2 before compression is extracted for the use in the lock hoppers.

Heat integration consists of steam generation for the gasifier and steam turbines. As shown in Fig. 3, although most steam is raised at HP conditions, additional IP steam is raised from lower-grade heat, mixed with the HP turbine exhaust, and the required process steam for the gasifier is then extracted at IP conditions. The remaining IP steam is expanded in two stages to the condenser pressure of 0.15 bar for power production.

3.1.3. *Gas switching integrated gasification with advanced gas treatment (GSIG-A)*

A diagram of this case is shown in Fig. 4 with the same gasifier setup as in the GSIG-B case. The same modelling approach of two separate Gibbs reactors representing gasification and GSC is employed. Advanced gas treatment starts with a cyclone to separate the ash from the gas, assumed to achieve 100% separation efficiency. Next, the syngas is cooled in a recuperative heat exchanger for desulphurization via adsorption on ZnO (with subsequent sorbent regeneration [39]), modelled as an H_2S separator operating at 400 °C. Such high temperature desulphurization is essential to prevent condensation of the tars to be cracked in the subsequent Ni-catalyzed tar cracker [40], modelled as an equilibrium reactor. For this, the gas is reheated to about 778 °C in

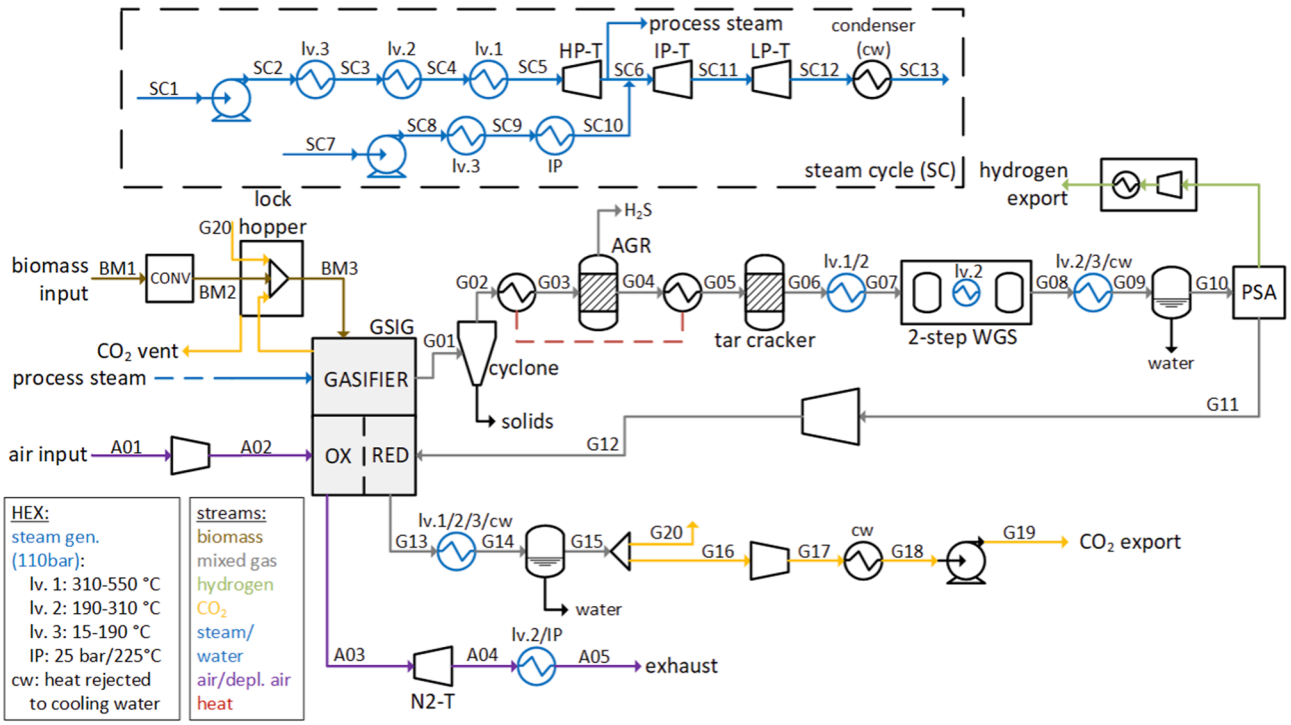

Fig. 4. Flow diagram of the GSIG process with advanced gas treatment.

the aforementioned recuperative heat exchanger and passed through a catalytic cracker to convert higher hydrocarbons to light components. Subsequently, a two-step water–gas-shift is implemented followed by a PSA with the off-gas integrated into the GSIG unit in the same way as in the GSIG-B case.

3.2. Economic assessment

The economic assessment was completed using the standardized economic assessment (SEA) tool [41], and the full SEA tool files for each case included in this paper are available online.[1] This tool offers a convenient platform for bottom-up economic assessments of novel processes, starting with capital cost assessments of all process units considered in the process simulation. Most of the equipment (turbomachines, heat exchangers, vessels) were assessed using the correlations of Turton, Bailie [42], while some specialized process units required the use of scaling correlations according to Eq. (1) and Table 3. Here, C is the bare erected cost of the process unit and S is the required scale. This cost is scaled from a reference unit with cost C_0 and scale S_0 using a given scaling exponent e to represent economies of scale for larger units.

$$C = C_0\left(\frac{S}{S_0}\right)^e \tag{1}$$

The estimation of the gasifier cost in the GSIG plants represents an important uncertainty in this study. For this purpose, the following methodology was employed. First, the gasifier cost was scaled to € in the year 2020 and the required 296.7 MW scale to arrive at a cost of 80.33 M€. Subsequently, costs related to the syngas coolers, quench, and water wash (heat exchangers and vessels calculated via Turton correlations [42]) were subtracted to arrive at an isolated gasifier bare erected cost of 63.23 M€. Subsequently, correlations for process vessels from Turton, Bailie [42] were used to estimate the cost of gasifier volume by assuming an expensive Ni-alloy liner on the inside, followed by an insulation layer and a carbon steel pressure shell on the outside. These vessels amounted to a cost of 14.46 M€ and the remaining 48.59 M€ was assumed to represent specific gasifier components such as the lock-hopper feed system, the ash removal system, cyclones/filters for particle separation, all the flanges and connections to the pressurized reactor volume, and the control system.

This cost of 48.59 M€ was kept constant for the GSIG gasifier, and the process vessel correlations were used to estimate the increase in cost due to additional reactor volume and all the GSC reactor tubes required inside the vessel. The added volume of the GSC tubes required the cross section of the gasifier to almost double. In addition, all the GSC tubes were added as Ni-alloy process vessels and doubled in cost to account for the complexity of the GSIG geometry. The diameter of the GSC tubes was determined to supply the required rate of heat transfer assuming a 300 $W/m^2/K$ heat transfer coefficient, resulting in about 180 tubes of 30 cm diameter. All these additional reactor volume costs combined with the cost of valves and oxygen carrier material made the GSIG gasifier in the GSIG-B case 77% more expensive than the reference.

When the bare erected costs of all equipment are determined, additional plant level costs are added to arrive at the total overnight cost as outlined in Table 4. Additional fixed and variable operating costs are subsequently determined.

Once all the costs are assembled, a cash flow analysis is carried out to calculate the levelized cost of hydrogen ($LCOH$) in Eq. (3) so that the net present value (NPV) in Eq. (2) amounts to zero. Here, ACF is the annualized cash flow, t is a given year in the plant lifetime starting when construction commences, n is the plant lifetime, i is the discount rate, ϕ is the capacity factor, P_{H_2} (kg/year) is the maximum production rate of hydrogen at 100% capacity factor, C_{VOM} (€/year) is the variable operating and maintenance costs under maximum production, $C_{Capital}$ (€/year) is the yearly capital expenses during the construction years, and C_{FOM} (€/year) is the annual fixed operating and maintenance costs.

$$NPV = \sum_{t=0}^{n} \frac{ACF_t}{(1+i)^t} \tag{2}$$

$$ACF_t = \phi \cdot (LCOH \cdot P_{H_2} - C_{VOM}) - C_{Capital} - C_{FOM} \tag{3}$$

[1] https://bit.ly/38N7nbi.

Table 3
Scaling parameters, reference costs, capacities and scaling exponents for use with Eq. (1).

Equipment	Scaling parameter	Reference cost (M€)	Reference capacity	Scaling exponent	Year	Ref.
ASU	Oxygen produced [kg/s]	66.20	25.48	0.67	2007	[43]
Gasifier including gas cooling and cleaning	Thermal input [MW]	95.00	482.8	0.67	2007	[43]
Selexol acid gas removal (H_2S)	Syngas flowrate [kmol/s]	32.75	5.44	0.67	2011	[44]
ZnO acid gas removal (H_2S)	Thermal input [MW]	46.60	1254.0	0.67	2018	[45]
Rectisol acid gas removal (CO_2 and H_2S)	Syngas flowrate [kmol/s]	43.58	2.48	0.67	2007	[43]
WGS and tar cracker	Syngas flowrate [kg/s]	9.54	1046.06	0.67	2007	[46]
Pressure swing adsorption	Inlet flowrate (kmol/s)	27.96	4.74	0.6	2007	[46]
Cooling water tower	Cooling water flowrate [ton/s]	1.88	1	1	2002	[47]
High temperature valves	Volume flowrate [m^3/s]	0.15	2	0.6	2014	[48]

Table 4
Economic evaluation assumptions [22,44,49,50].

Capital estimation methodology		
Bare Erected Cost (BEC)	SEA Tool Estimate	
Engineering Procurement and Construction (EPC)	10% BEC	
Project Contingency (PC)	20% (BEC + EPC)	
Owners Costs (OC)	15% (BEC + EPC + PC)	
Total Overnight Costs (TOC)	BEC + EPC + PC + OC	
Operating & maintenance costs		
Fixed		
Maintenance	2.5	%TOC
Insurance	1	%TOC
Labour	60,000	€/y-p
Operators	50	Persons
Variable		
Biomass	7	€/GJ
Electricity	60	€/MWh
Oxygen carrier	15	$/kg
CO_2 transport & storage	20	€/ton
CO_2 tax	100	€/ton
Process water	6	€/m^3
Cooling water make-up	0.35	€/m^3
Cash flow analysis assumptions		
1st year capacity factor	65	%
Remaining years	85	%
Discount Rate	8	%
Construction period	3	years
Plant Lifetime	25	years

3.3. Performance metrics

Three technical performance measures are used in the discussion of the results. First, the hydrogen (Eq. (4)) and electric (Eq. (5)) efficiencies (η) are determined from the ratio of output to input energy, using lower heating values (LHV in MJ/kg) to represent chemical potential energy. Here, $\dot{m}_{H_2}$ and $\dot{m}_{BM}$ (kg/s) are the mass flow rates of hydrogen and biomass, respectively, whereas W_{El} (MW) is the net electricity production of the plant.

$$\eta_{H_2} = \frac{\dot{m}_{H_2} \bullet \mathrm{LHV}_{H_2}}{\dot{m}_{BM} \bullet \mathrm{LHV}_{BM}} \tag{4}$$

$$\eta_{El} = \frac{W_{El}}{\dot{m}_{BM} \bullet \mathrm{LHV}_{BM}} \tag{5}$$

Furthermore, the CO_2 capture ratio is quantified as the fraction of the carbon in the incoming biomass that is contained in the biomass that is exported from the process in the CO_2 stream for storage (Eq. (6)). Here, $\dot{n}_C$ (mol/s) is the molar flowrate of carbon.

$$CR = \frac{\dot{n}_{C,\,export}}{\dot{n}_{C,\,input}} \tag{6}$$

For the economic assessment, the LCOH (Eq. (3)) is the primary performance indicator. It is also broken down into sub-components for a richer discussion by dividing annualized costs in different categories by the amount of hydrogen produced in one year.

4. Results and discussion

Results will be presented and discussed in three parts: 1) techno-economic results from the three main cases, 2) the effect of changes to the GSIG gasifier operating temperatures, and 3) a sensitivity analysis to the most influential economic assumptions.

4.1. Base case results

Fig. 5 presents the results for the three main process configurations: the HTW benchmark (Fig. 2), the GSIG configuration with simplified gas treatment similar to the HTW plant (GSIG-B, Fig. 3), and the GSIG configuration with advanced gas treatment (GSIG-A, Fig. 4). Details about mass and energy flows in the different process configurations are provided in Table 5.

The main economic output is the levelized cost of hydrogen (LCOH) shown in Fig. 5a. All plants have relatively high hydrogen production costs of 3 €/kg or higher. Biomass-to-hydrogen routes are relatively expensive due to the processing of a challenging and relatively expensive solid fuel without great economies of scale. Hence, the costs to produce hydrogen is much higher than large-scale fossil fuel alternatives. However, Fig. 5a shows that over half of this cost is cancelled out by the 100 €/ton credit assumed for storing the biogenic CO_2 captured from the process. This large CO_2 credit results in an attractive LCOH in the range of 1.31–1.64 €/kg. The 5.2%-points higher CO_2 capture ratio facilitated by the GSIG concept (Fig. 5c) is a considerable benefit in this respect, increasing the revenues from the CO_2 credit. On a levelized basis, however, the CO_2 credit in the GSIC gases is smaller than the HTW benchmark (Fig. 5a) because the CO_2 credit is levelized over a 7.5–12.2% higher hydrogen output.

Under the base assumptions, the GSIG-B configuration achieves a 5% reduction in LCOH relative to the HTW benchmark. This saving results from the increase in H_2 production efficiency (Fig. 5c) facilitated by the GSIG concept where the low-grade PSA off-gas fuel is efficiently used to supply the heat required for the endothermic steam gasification instead of being combusted for low-efficiency power production with associated CO_2 emissions. As Fig. 5b shows, however, the GSIG-B plant is more costly to construct than the HTW benchmark because the much more expensive gasifier cancels out the benefits of avoiding the ASU and a separate CO_2 capture process (included as AGR in Fig. 5b). The need to compress and expand air for the GSC tubes also increase turbomachinery costs. Despite these higher capital costs, Fig. 5a shows that the levelized capital cost remains marginally lower than that of the HTW benchmark because of the 7.5% greater hydrogen output facilitated by the improved process efficiency.

Advanced gas treatment in the GSIG-A case leads to a further 12% reduction in LCOH relative to the GSIG-B case. Savings arise mainly from higher electric and power generation efficiencies. As Fig. 5c shows, advanced gas treatment transforms the plant from an electricity importer to a slight electricity exporter. This large electricity saving substantially reduces the variable operating and maintenance (VOM)

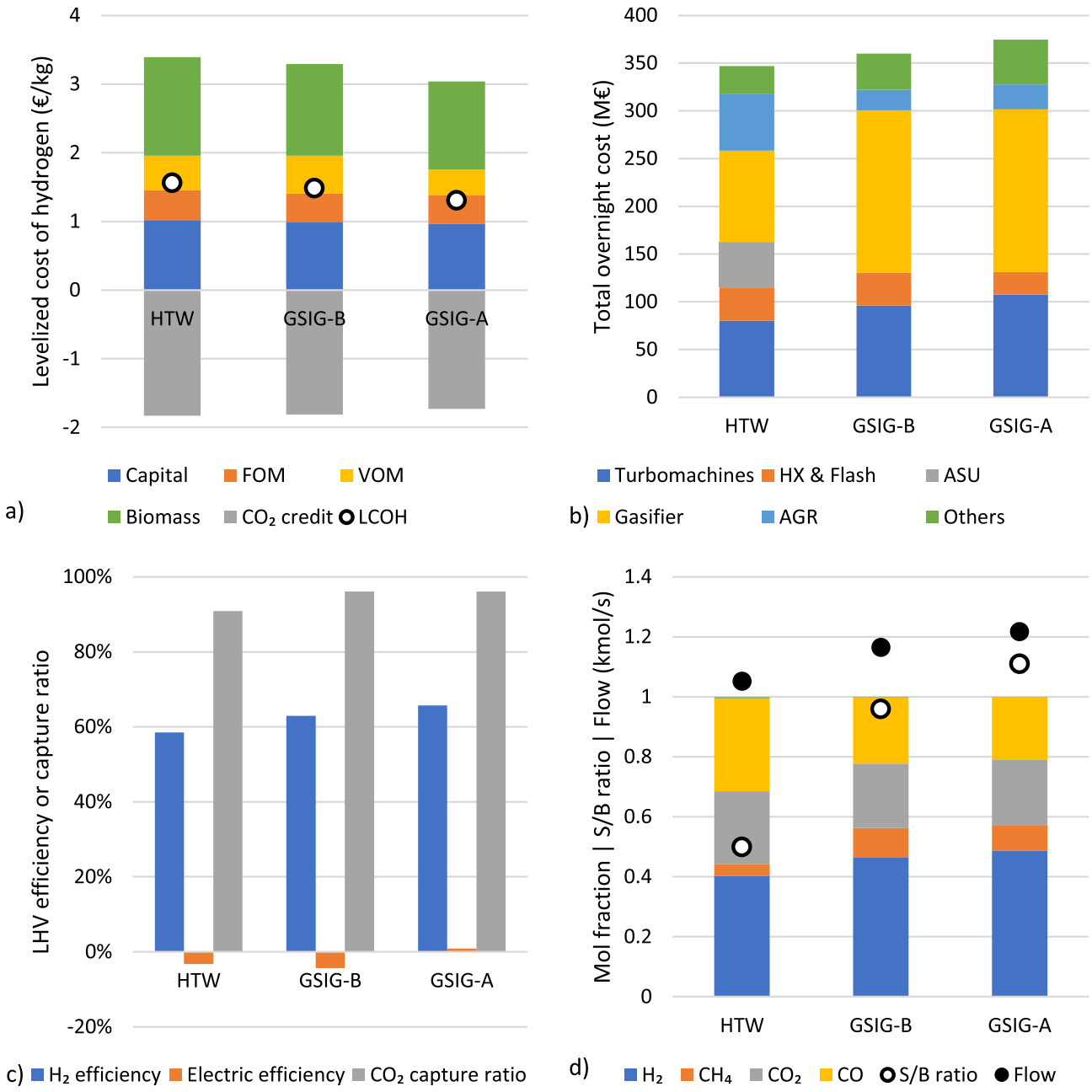

Fig. 5. Techno-economic results for the three main process configurations. Detailed assessments of each case can be viewed in the individual economic assessment files available online[1]. [1]https://bit.ly/38N7nbi.

costs in Fig. 5a. The increase in electric efficiency comes from much larger steam turbine power output because the relatively high-grade thermal energy that was rejected in the quenching and water wash steps in the GSIG-B plant can now be recovered and used to drive the power cycle. Fig. 5b shows that these larger steam turbines increased the turbomachinery cost, but that this cost increase is cancelled out by a reduction in flash vessel cost (the quench and water wash were costed as large flash vessels). The tar cracker also increased equipment costs in the GSIG-A case.

Finally, Fig. 5d shows how the dry syngas composition directly after the gasifier and S/B ratio changes between the three cases. The HTW benchmark produces a syngas with relatively little CH_4 and more CO at a lower S/B ratio because of the addition of O_2 to the gasifier and the higher gasification temperature. The oxycombustion used to supply the heat for gasification in this configuration produces significant amounts of CO_2 as a gasification agent, increasing CO yields, and the higher temperature inhibits CH_4 formation due to reaction equilibrium considerations. The GSIG cases show a significant change in the syngas composition. The absence of O_2 requires more steam to be added as a gasification agent, resulting in a syngas containing more H_2 and less CO. Furthermore, the lower gasification temperature (800 °C) results in a substantial fraction of CH_4 in the syngas. The 10% CH_4 share in the syngas in the GSIG-B case represents 28% of its LHV, which would be a problem for conventional processes because this is a large fraction of energy that cannot be recovered as H_2 in the downstream processing units. However, the GSIG process requires a considerable amount of fuel heating value for combustion in the GSC tubes to supply the gasification energy, allowing the CH_4 to be efficiently utilized. The GSIG-A case requires a higher S/B ratio than the GSIG-B case where the large amount of water added in the quench facilitates a greater shift of CO to H_2 in the WGS reactors. The GSIG cases also produce a higher syngas flowrate as the indirect heat supply allows more H_2 and CO to be produced from the

Table 5
Mass and energy flows for the three main process configurations.

Case	HTW	GSIG-B	GSIG-A	
Mass flows				
Biomass input	15.00	15.00	15.00	kg/s
H_2 output	1.31	1.41	1.47	kg/s
CO_2-rich stream	24.04	26.46	26.46	kg/s
CO_2 purity	100.00	96.70	96.40	%
CO_2 capture ratio	90.89	96.08	96.11	%
Heat flows (LHV)				
Biomass heat input	269.66	269.66	269.66	MW
H_2 heat output	157.83	169.76	177.12	MW
H_2 efficiency	58.53	62.95	65.68	%
Electric efficiency	−3.25	−4.38	0.85	%
Electricity flows				
Water pumps	−1.19	−1.06	−0.78	MW
H_2 compressor	−2.72	−2.86	−3.32	MW
CO_2 compressors & pump	−9.84	−3.37	−3.64	MW
ASU	−7.13			MW
AGR	−3.95			MW
Steam turbines	16.06	6.30	21.37	MW
Air compressors		−19.06	−18.14	MW
Recycle compressor		−13.03	−13.27	MW
N_2 turbine		21.28	20.07	MW
Net power	−8.77	−11.80	2.29	MW

steam gasification of the biomass. A higher S/B ratio in the GSIG-A case further increases the flowrate as some CH_4 is steam-reformed to H_2 and CO.

4.2. GSIG gasifier operating temperatures

As illustrated in Fig. 6a, raising the temperature in the GSC tubes (three cases on the left) or in both the gasifier and the GSC tubes (three cases on the right) only had a minor effect on the economic performance of the GSIG plant. Fig. 6b shows that the main effect of increasing the temperature is an exchange of lower hydrogen production efficiency for higher electrical efficiency. A higher GSC operating temperature produces outlet streams containing more thermal energy that can be recovered more efficiently in the gas and steam turbines at the expense of having to combust more fuel in the GSC reactors. A higher gasifier temperature allows for the use of a lower S/B ratio to produce the amount of hydrogen that can be extracted in the PSA while leaving enough heating value in the PSA off-gas for combustion in the GSC tubes. Thus, more steam can be used in the power cycle, but the gasification reaction becomes more endothermic as less methane is formed, requiring more fuel to be combusted in the GSC tubes instead of being extracted as hydrogen in the PSA.

This trade-off contributes to keeping the LCOH essentially constant in the cases where the gasifier and GSC tube temperatures are increased simultaneously. Capital costs also increase in this case because of the more endothermic gasification reactions that increase the required volume and surface area of the GSC tubes. On the other hand, the cases where only the GSC tube temperature is increased (higher tube-gasifier ΔT) slightly reduced the gasifier cost and the LCOH due to a lower GSC tube surface area facilitated by the larger driving force for heat transfer.

An important uncertainty is the effect of higher gasifier temperatures on gasifier capital cost. This effect was ignored in the present study, keeping the gasifier cost (excluding GSC tubes) constant with increasing gasifier temperature, but there are several complex competing effects to consider in practice. Higher gasifier temperatures will increase reaction rates that will reduce the required biomass residence time in the gasifier, although this effect will be moderated by the increased importance of the bubble-to-emulsion mass transfer resistance present in fluidized beds. On the other hand, lower temperatures may facilitate the use of lower cost construction materials and will reduce the volume of gas to be handled.

As mentioned in the prior discussion around Fig. 5d, the high presence of methane in the syngas from relatively low-temperature operation at 800 °C is not a problem in the GSIG configuration because the heating value in the methane can be efficiently exploited in the GSC tubes. Thus, it may be possible to operate the gasifier even at temperatures below 800 °C with little or no economic penalty if the biomass reactivity remains sufficiently high. Such low-temperature operation may improve the longevity of the internal surfaces required for heat transfer in the GSIG unit.

4.3. Sensitivity analysis

The variation of the levelized cost of hydrogen to changes in six key parameters is illustrated in Fig. 7. Biomass and CO_2 prices are the most influential variables. The interplay between these two variables will be crucial factor in future decades as decarbonization becomes an ever-increasing priority. As Fig. 7c illustrates, higher CO_2 prices can make hydrogen from biomass extremely attractive. In Europe, CO_2 prices of 150 €/ton and beyond will be required to achieve net-zero by 2050. For example, the latest IEA World Energy Outlook sees levels of 120, 170, and 200 $/ton by 2030, 2040, and 2050, respectively, in advanced economies with net-zero pledges.

Such high CO_2 prices will greatly increase the demand for BECCS technologies like the biomass-to-H_2 pathways investigated in this paper. Since sustainable biomass is a limited resource, such a scenario will soon drive up biomass prices, incentivising the market to produce more biomass. For a technology with a high CO_2 capture ratio like GSIG, a 10 €/ton increase in the CO_2 credit received for storing biogenic CO_2 can cancel out a biomass price increase of about 1 €/GJ. Thus bio-derived H_2 can be produced at a competitive cost of around 1.5 €/kg at CO_2 prices beyond 150 €/ton even if biomass prices rise above 12 €/GJ. Such a scenario should be carefully regulated as it could incentivise unsustainable exploitation of biomass resources.

Fig. 7b shows a much smaller effect of the electricity price. However, higher electricity prices clearly favour the GSIG-A configuration where advanced gas treatment allows more heat to be recovered for use in the power cycle. Although current large European consumers pay prices around 60 €/MWh [51], a rapid decarbonization effort is likely to significantly increase electricity prices, so this is an important benefit. For example, at an electricity price of 120 €/MWh, GSIG-A is 20% cheaper than the GSIG-B.

The sensitivity to gasifier cost in Fig. 7d shows the importance of the uncertainty in estimating the cost of the GSIG gasifier illustrated in Fig. 1. Since volume and surface area of the GSC tubes impose considerable additional costs, the GSIG gasifier is substantially more costly than the conventional benchmark. Hence, a gasifier cost increase of 50% almost cancels out the advantage of the GSIG concept (comparing the HTW and GSIG-B cases with similar gas treatment). When only considering cost increases in the GSIG gasifier with the reference gasifier cost kept constant (dashed line in Fig. 7d), a 13% increase is sufficient to cancel out the economic advantage of the GSIG-B case relative to the benchmark. Put another way, the GSIG gasifier is 77% more expensive than the conventional gasifier under base-case assumptions, but the advantage in terms of LCOH is lost when this cost increase rises to 100%.

Due to this sensitivity, minimizing the GSIG gasifier cost is essential for its commercial prospects. As discussed around Fig. 6, the gasification temperature presents an interesting optimization lever to explore since lower operating temperatures can allow cheaper construction materials than those assumed in this assessment at the expense of a larger reactor volume. Further savings could be achieved by maximizing the gas throughput in the GSC tubes to reduce the volume they occupy within the gasifier as a relatively conservative superficial velocity of 0.6 m/s was employed in this assessment.

While the gasifier cost uncertainty strongly influences the GSIG cases, Fig. 7e shows that the reference HTW case is more sensitive to ASU and AGR cost assumptions. The GSIG configurations avoid the ASU and the CO_2 capture unit, substantially reducing uncertainty related to

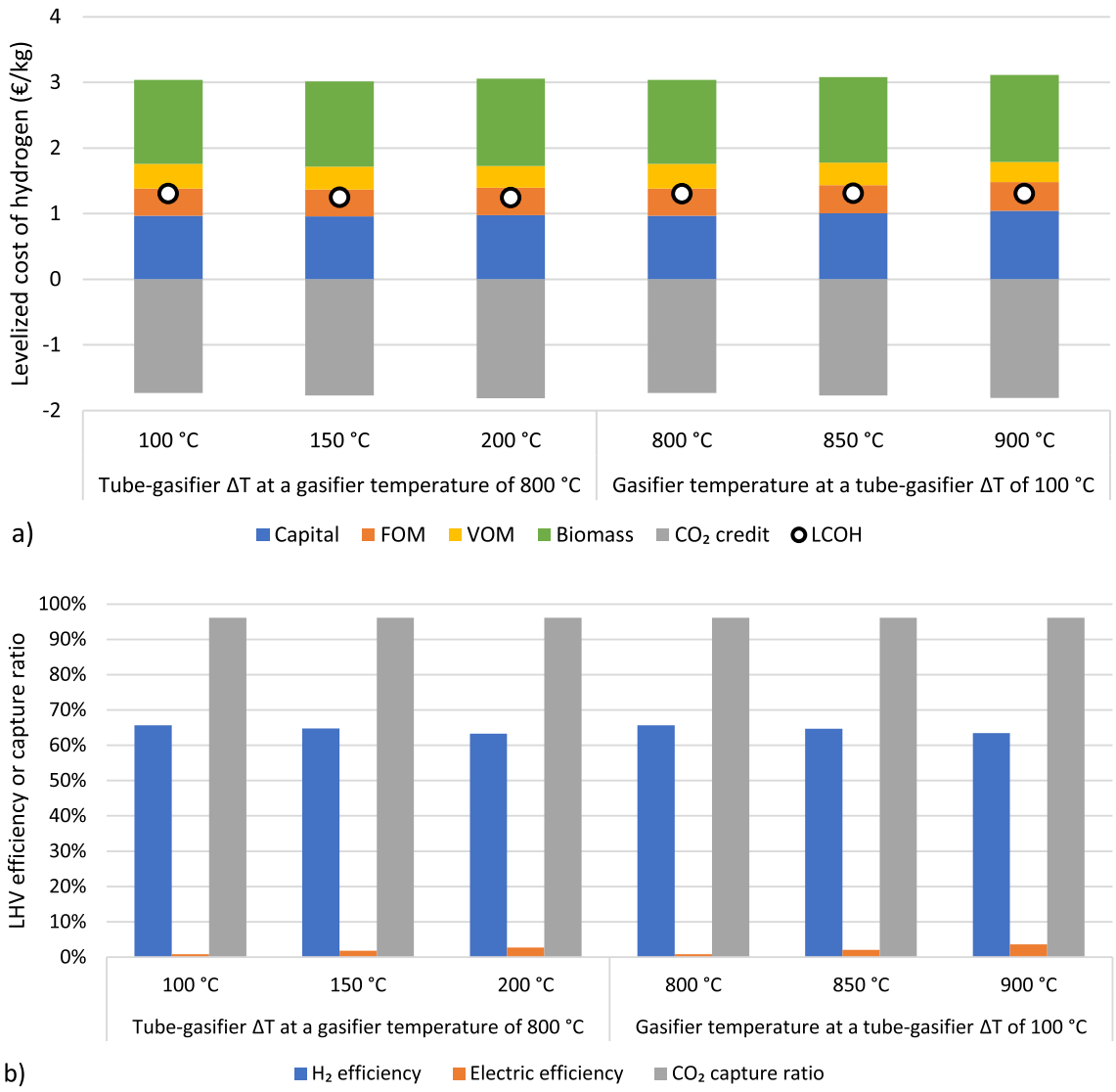

Fig. 6. Techno-economic results for the GSIG-A case when increasing the difference between the gasifier and GSC tube temperatures (left) and when increasing the gasifier and tube temperatures simultaneously (right).

these process units.

Finally, Fig. 7f shows the effect of plant availability on the LCOH. Since the three plants have similar specific capital costs, the response to changes in capacity factor are also similar. The novel GSIG gasifier may lead to more downtime (at least for initial plants), and the dashed line in Fig. 7f shows that the LCOH advantage relative to the HTW plant at 85% capacity factor is lost if the GSIG-B plant capacity factor falls to 80%.

5. Summary and conclusions

This study investigated the techno-economic performance of the novel gas switching integrated gasification (GSIG) concept for hydrogen production from biomass with integrated CO_2 capture. The GSIG concept was benchmarked against a conventional O_2-blown fluidized bed gasifier with pre-combustion CO_2 capture to assess its potential for future development.

The key novelty of GSIG is combustion of the pressure swing adsorption (PSA) off-gas fuel with inherent CO_2 separation in tubular gas switching combustion (GSC) reactors integrated into the gasifier. This integration allows GSIG to avoid the need for an air separation unit and a dedicated CO_2 capture facility, improving efficiency and CO_2 avoidance. On the other hand, the gasifier becomes considerably larger and more complex.

Process modelling revealed that the GSIG concept can boost hydrogen production by 7.5% and CO_2 capture by 5.2%-points relative to the benchmark. Capital costs increased by 3.5% as higher gasifier costs outweighed the avoidance of the ASU and CO_2 capture unit. In terms of economic performance, these results facilitated a 5.1% reduction in the levelized cost of hydrogen (LCOH). Advanced gas treatment to handle tars using a tar cracker instead of a water wash further improved efficiency and eliminated the need for electricity imports to achieve a further LCOH reduction of 12.0%.

Although the GSIG gasifier is more complex, one mitigating feature is that lower temperature gasification can be efficiently facilitated because the higher fraction of methane forming under such conditions can be efficiently combusted in the GSC tubes for heat supply. Due to this feature, raising the gasifier temperature from 800 to 900 °C did not significantly change the LCOH.

The combination of relatively high capital costs and expensive fuel results in high hydrogen production costs in in excess of 3 €/kg. However, a CO_2 credit of 100 €/ton for negative emissions offsets more than half of this cost to result in an attractive LCOH ranging from 1.31 €/kg for GSIG with advanced gas treatment to 1.64 €/kg for the conventional benchmark with standard gas treatment. Even higher CO_2 credits, which

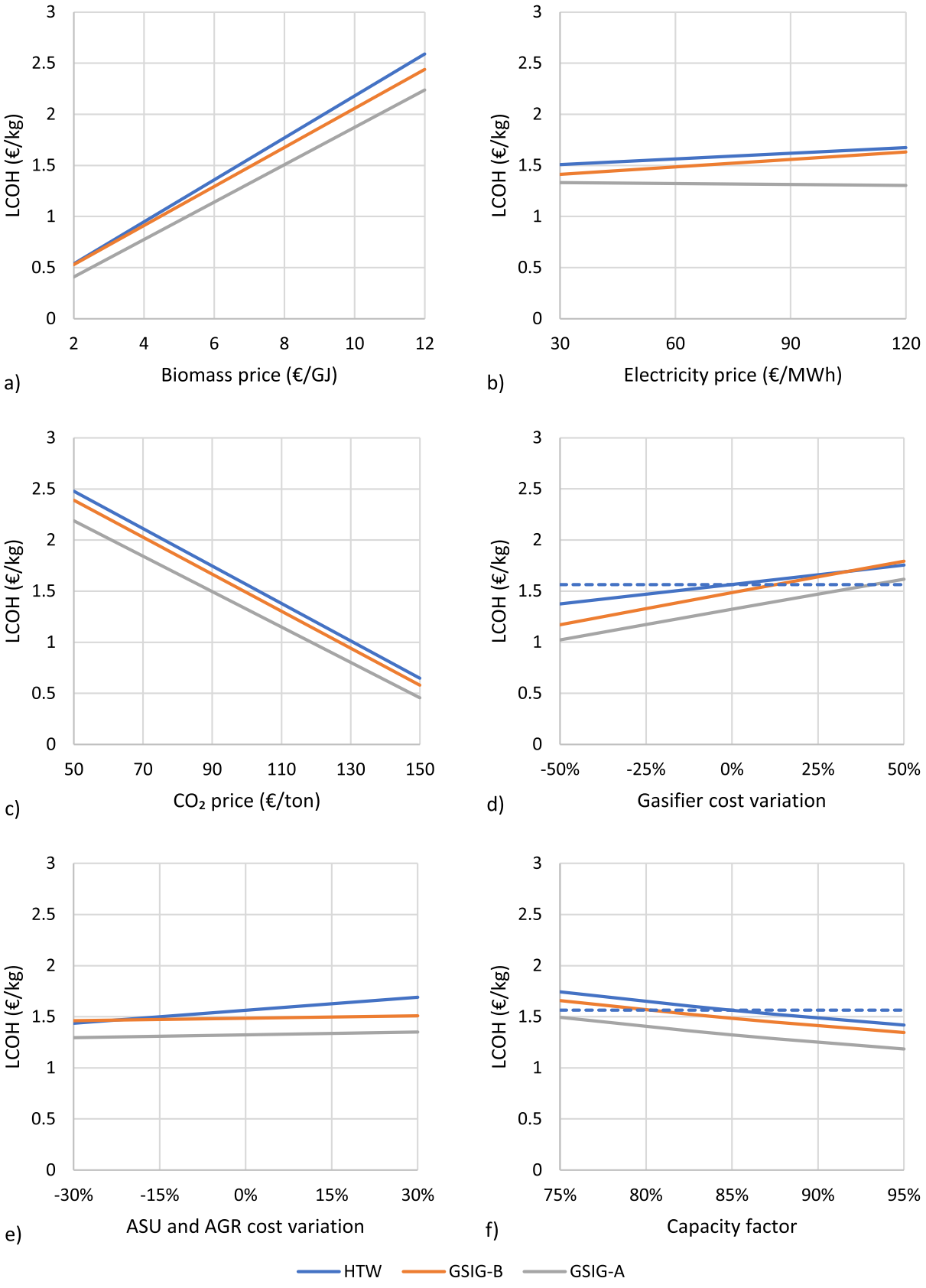

Fig. 7. Sensitivity of the levelized cost of hydrogen to changes in four influential economic assumptions. Central levels of the variables are specified in Table 4.

would be required in ambitious decarbonization scenarios, result in extremely low LCOH values that will incentivise large consumption of biomass. Such a scenario requires careful regulation to prevent unsustainable biomass exploitation.

Overall, biomass-to-hydrogen with CO_2 capture appears well positioned for economically achieving negative CO_2 emissions in a rapidly decarbonizing world. The GSIG concept can significantly enhance the efficiency with which the limited biomass resource is utilized and potentially create significant economic benefits. Dedicated experimental demonstration activities are therefore recommended to reduce uncertainty related to the novel gasifier design.

CRediT authorship contribution statement

Antonia Helf: Investigation, Methodology, Visualization, Writing – original draft. **Schalk Cloete:** Conceptualization, Methodology, Formal analysis, Investigation, Visualization, Supervision, Writing – original draft. **Florian Keller:** Supervision, Writing – original draft. **Jan Hendrik Cloete:** Writing – original draft. **Abdelghafour Zaabout:** Funding acquisition, Project administration.

Declaration of Competing Interest

The authors declare that they have no known competing financial interests or personal relationships that could have appeared to influence the work reported in this paper.

Data availability

Data will be made available on request.

References

[1] IPCC, *Climate Change 2021: The Physical Science Basis*. 2021.
[2] van der Spek M, et al. Perspective on the hydrogen economy as a pathway to reach net-zero CO2 emissions in Europe. Energy Environ Sci 2022.
[3] International Energy Agency, *Energy Technology Perspectives 2020*. 2020, International Energy Agency: Paris.
[4] Voldsund M, Jordal K, Anantharaman R. Hydrogen production with CO2 capture. Int J Hydrogen Energy 2016;41(9):4969–92.
[5] Buttler A, Spliethoff H. Current status of water electrolysis for energy storage, grid balancing and sector coupling via power-to-gas and power-to-liquids: A review. Renew Sustain Energy Rev 2018;82:2440–54.
[6] Msheik M, Rodat S, Abanades S. Methane Cracking for Hydrogen Production: A Review of Catalytic and Molten Media Pyrolysis. Energies 2021;14(11):3107.
[7] Hilaire J, et al. Negative emissions and international climate goals—learning from and about mitigation scenarios. Clim Change 2019;157(2):189–219.
[8] IPCC, *Global Warming of 1.5°C*. 2018, Intergovernmental Panel on Climate Change.
[9] Erans M, et al. Direct air capture: process technology, techno-economic and socio-political challenges. Energy Environ Sci 2022.
[10] Kemper J. Biomass and carbon dioxide capture and storage: A review. Int J Greenhouse Gas Control 2015;40:401–30.
[11] Arodudu O, Holmatov B, Voinov A. Ecological impacts and limits of biomass use: a critical review. Clean Technol Environ Policy 2020;22(8):1591–611.
[12] Heck V, et al. Biomass-based negative emissions difficult to reconcile with planetary boundaries. Nat Clim Change 2018;8(2):151–5.
[13] Lepage T, et al. Biomass-to-hydrogen: A review of main routes production, processes evaluation and techno-economical assessment. Biomass Bioenergy 2021;144:105920.
[14] Karl J, Pröll T. Steam gasification of biomass in dual fluidized bed gasifiers: A review. Renew Sustain Energy Rev 2018;98:64–78.
[15] Hofbauer H, et al. Biomass CHP plant Güssing - a success story. In: Bridgwater AV, editor. Pyrolysis Gasification Biomass Waste. Newsbury, UK: CPL Press; 2003. p. 371–83.
[16] Nazir SM, et al. Efficient hydrogen production with CO2 capture using gas switching reforming. Energy 2019;185:372–85.
[17] Williams RH, et al. Methanol and hydrogen from biomass for transportation. Energy for Sustainable Development 1995;1(5):18–34.
[18] Karellas S, Karl J, Kakaras E. An innovative biomass gasification process and its coupling with microturbine and fuel cell systems. Energy 2008;33(2):284–91.
[19] Wang Y, et al. Techno-economic analysis of biomass-to-hydrogen process in comparison with coal-to-hydrogen process. Energy 2019;185:1063–75.
[20] Salkuyeh YK, Saville BA, MacLean HL. Techno-economic analysis and life cycle assessment of hydrogen production from different biomass gasification processes. Int J Hydrogen Energy 2018;43(20):9514–28.
[21] Rauch R, Hrbek J, Hofbauer H. Biomass gasification for synthesis gas production and applications of the syngas. WIREs Energy Environ 2014;3(4):343–62.
[22] Adanez J, et al. Progress in Chemical-Looping Combustion and Reforming technologies. Prog Energy Combust Sci 2012;38(2):215–82.
[23] Zhao X, et al. Biomass-based chemical looping technologies: the good, the bad and the future. Energy Environ Sci 2017;10(9):1885–910.
[24] Osman M, et al. Review of pressurized chemical looping processes for power generation and chemical production with integrated CO2 capture. Fuel Process Technol 2021;214:106684.
[25] Ugwu A, et al. Gas switching technology: Economic attractiveness for chemical looping applications and scale up experience to 50 kWth. Int J Greenhouse Gas Control 2022;114:103593.
[26] Zaabout A, Cloete S, Amini S. Autothermal operation of a pressurized Gas Switching Combustion with ilmenite ore. Int J Greenhouse Gas Control 2017;63:175–83.
[27] Zaabout A, et al. A pressurized Gas Switching Combustion reactor: Autothermal operation with a CaMnO3−δ-based oxygen carrier. Chem Eng Res Des 2018;137:20–32.
[28] Arnaiz del Pozo C, et al. The potential of chemical looping combustion using the gas switching concept to eliminate the energy penalty of CO2 capture. Int J Greenhouse Gas Control 2019;83:265–81.
[29] Arnaiz del Pozo C, et al. Integration of gas switching combustion in a humid air turbine cycle for flexible power production from solid fuels with near-zero emissions of CO2 and other pollutants. Int J Energy Res 2020;44(9):7299–322.
[30] Arnaiz del Pozo C, et al. Integration of gas switching combustion and membrane reactors for exceeding 50% efficiency in flexible IGCC plants with near-zero CO2 emissions. Energy Conversion and Management: X 2020;7:100050.
[31] Szima S, et al. Techno-Economic Assessment of IGCC Power Plants Using Gas Switching Technology to Minimize the Energy Penalty of CO2 Capture. Clean Technologies 2021;3(3):594–617.
[32] Szima S, et al. Finding synergy between renewables and coal: Flexible power and hydrogen production from advanced IGCC plants with integrated CO2 capture. Energy Convers Manage 2021;231:113866.
[33] Wassie SA, et al. Hydrogen production with integrated CO2 capture in a novel gas switching reforming reactor: Proof-of-concept. Int J Hydrogen Energy 2017;42(21):14367–79.
[34] Nazir SM, et al. Pathways to low-cost clean hydrogen production with gas switching reforming. Int J Hydrogen Energy 2020.
[35] Szima S, et al. Gas switching reforming for flexible power and hydrogen production to balance variable renewables. Renew Sustain Energy Rev 2019;110:207–19.
[36] Cloete S, Hirth L. Flexible power and hydrogen production: Finding synergy between CCS and variable renewables. Energy 2020;192:116671.
[37] Arnaiz del Pozo C, et al. The oxygen production pre-combustion (OPPC) IGCC plant for efficient power production with CO2 capture. Energy Convers Manage 2019;201:112109.
[38] Wolfersdorf C, et al. CO2-to-X and Coal-to-X Concepts in Pulverized Coal Combustion Power Plants. Energy Procedia 2017;114:7171–85.
[39] Denton, D.L., An update on RTI's warm syngas cleanup demonstration project, in Gasification Technologies Conference. 2014: Washington, DC.
[40] Dayton, D., *A Review of the Literature on Catalytic Biomass Tar Destruction*. 2002, National Renewable Energy Laboratory.
[41] Arnaiz del Pozo, C., S. Cloete, and Á. Jiménez Álvaro. *Standard Economic Assessment (SEA) Tool. Available from: https://bit.ly/3IXPWC8*. 2021.
[42] Turton, R., et al., *Analysis, synthesis and design of chemical processes: Appendix A*. 2008: Pearson Education.
[43] Liu G, et al. Making Fischer−Tropsch Fuels and Electricity from Coal and Biomass: Performance and Cost Analysis. Energy Fuels 2011;25(1):415–37.
[44] Franco, F., et al., European Best Practice Guidelines for CO2 Capture Technologies, in CESAR project: European Seventh Framework Programme. 2011.
[45] Arnaiz del Pozo C, Cloete S, Jiménez Álvaro Á. Carbon-negative hydrogen: Exploring the techno-economic potential of biomass co-gasification with CO2 capture. Energy Convers Manage 2021;247:114712.
[46] Spallina V, et al. Techno-economic assessment of membrane assisted fluidized bed reactors for pure H2 production with CO2 capture. Energy Convers Manage 2016;120:257–73.
[47] EPRI, *Cooling System Retrofit Cost Analysis*. 2002: Palo Alto, CA.
[48] Hamers HP, et al. Comaprison on process efficiency for CLC of syngas operated in Packed Bed and Fluidized Bed Reactors. Int J Greenhouse Gas Control 2014;28:65–78.
[49] S2BIOM, *S2BIOM integrated tool set*. 2022, https://s2biom.wenr.wur.nl/web/guest/home.
[50] Rubin, E., et al., *Toward a common method of cost estimation for CO2 capture and storage at fossil fuel power plants*. 2013, Global CCS institute.
[51] CREG, *A European comparison of electricity and gas prices for large industrial consumers*. 2020, PwC Enterprise Advisory.